Cent. Eur. J. Biol. • 5(2) • 2010 • 197-213
DOI: 10.2478/s11535-009-0068-3

VERSITA

Central European Journal of **Biology**

Digital control circuitry for the p53 dynamics in cancer cell and apoptosis

Research Article

Rosario M. Ardito Marretta*

Department of Structural, Aerospace Engineering and Geotechnics,
University of Palermo,
90128 Palermo, Italy

Received 4 June 2009; Accepted 4 September 2009

Abstract: Experimental work and theoretical models deduce a "digital" response of the p53 transcription factor when genomic integrity is damaged. The mutual influence of p53 and its antagonist, the Mdm2 oncogene, is closed in a feedback. This paper proposes an aerospace-based architecture for translating the p53/Mdm2/DNA damage network into a digital circuitry in which the optimal control theory is applied for obtaining the requested dynamic evolutions of some considered cell species for repairing a DNA damage. The purpose of this paper is to demonstrate the usefulness of such digital circuitry design to detect and predict the cell species dynamics for shedding light on their inner and mutual mechanisms of interaction. Moreover, the cell fate is newly conceived by the modified pulsing mechanism of p53 and other apoptotic species when the digital optimal control is applied to an apoptosis wiring diagram.

Keywords: *p53 • Cellular circuitry • Feedback control • Protein networks signalling • Apoptosis*

1. Introduction

There is remarkable and increasing cooperation between biology and mathematics due in part to the decoding of the human genome [1-10]. Since its discovery, the oncosuppressor p53 protein has been suggested to play a prominent role in the evolution of a cancer cell. p53 activation and concentration increase are the main responses to aberrant oncogene signals. p53 is also capable of inducing the transcription of genes in charge of the cell-cycle arrest, DNA repair and apoptosis [11-15]. Some studies [16] have addressed the idea that increased expression of p53 in damaged cells may be explained by more than one mechanism. Clinically validated anticancer drugs can inhibit the function of oncoproteins leading to tumour regression depending on the cancer type with the main result of p53 restoration [17]. Bates *et al.* [18] propose a model in which E2F-1 (a protein inherently activated by cell-cycle progression) in conjunction with another protein ($p14^{ARF}$), protects cells against oncogenic changes and aberrant cell proliferation. A recent work [19] not only confirms that p53 is inhibitory *in vivo* but also demonstrates that its activation is required for the pro-apoptotic target gene binding protein called IGFBP3. These conclusions are directly related to a previous study [20] which showed that, at physiological temperatures, wild-type p53 was more than 50% unfolded with a 75% loss in DNA-binding activity. Although these works can be considered milestones from a purely biological point of view, so far they have not been utilized mathematically.

The guidelines of the present paper are those given by recent literature [11-15,21-24] in which the p53/Mdm2 feedback loop is mathematically described for a human single-cell proteins dynamics. These studies conclude that p53 can be expressed into a series of discrete pulses after DNA damage and the p53/Mdm2 network system is *in toto* constrained by a feedback loop and (potentially) expressed by digital layers. These studies show different and almost conflicting points of view in terms of output amplitudes, frequencies, interpulses and other oscillation parameters of the p53/Mdm2 dynamic responses. In short, a negative feedback loop generates damped oscillations, while schemes such as

* *E-mail: romario@unipa.it*

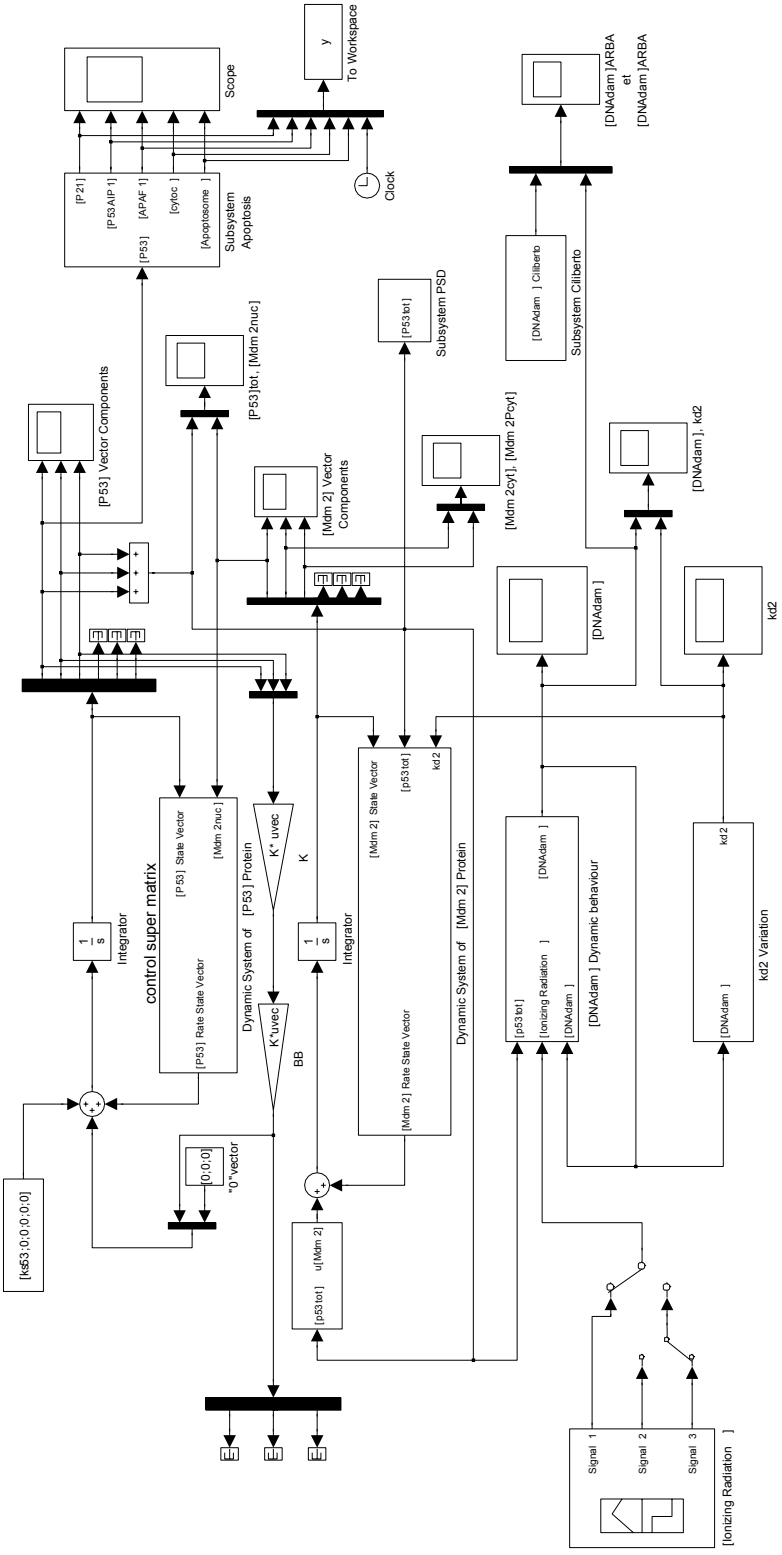

Figure 1. Human cell digital circuitry with control matrix - according to the employed block diagram algebraic definition, we have: integrator block (it digitally performs the solution of integral expressions, e.g., $\int x dx = x^2/2$); "0" vector block is a zero-elements vector; BB is a matrix block that is employed to build up the control matrix feedback, K, in the LQR system (see Appendix); kd2 block digitally performs the rate constant for degradation of Mdm2nuc; PSD subsystem block performs the Power Spectral Density analysis.

positive feedback loops of p53 may enhance undamped dynamics.

An important contribution for understanding the dynamics and variability of p53/Mdm2 system was given by Geva-Zatorsky *et al.* [12]. They evaluated the amplitude and width of each peak of nuclear Mdm2-YFP (yellow-fluorescent-protein) and calculated the average of these properties. Ultimately, those authors obtained prolonged undamped oscillations in the p53/Mdm2 system.

Batchelor *et al.* [24] draw the conclusion that the p53/Mdm2 negative feedback loop is described by the interaction of two different timescales: a slow positive transcriptional arm and a fast negative protein-protein interaction arm. Their results show that the p53/Mdm2 feedback loop does not - by itself - drive sustained p53 oscillations. Thus, they identify the wild type p53-induced phosphatase 1, Wip1, as the central element mediating a second (negative) feedback loop for chaining p53 and the upstream signalling proteins. Since the response of p53/Mdm2 system to a DNA damage can be digitally described, mathematical models - based on a set of differential equations - can be reliable to predict the mutual influence of p53/Mdm2/DNA_{dam} network. Therefore, this study focused on A) the p53 protein role within a human single-cell scheme; B) the digital signalling of the mutual interaction between p53 and Mdm2 when DNA is altered and, C) a dynamic control of this proteins kinase by digital system layers.

Even though the mathematical methods based on a set of ordinary differential equations (ODEs) are quite well capable to describe the cell proteins and species time-dependent interactions, they are confined in the cell behavior and evolution in “itself”. In other words, the mathematical methods describe the actual cell dynamics which may or may not involve DNA damage, *i.e.*, the mathematical approach remains only a “witness” of the considered cell protein interactions. Conversely, through a human cell digital scheme, it is possible to identify and/or detect more effective species and kinases, concentration and timescale dynamics to achieve faster and modified evolutions of DNA repairing. Reproducibility of the proposed methods by molecular biologists and genetic engineering manipulations could be helpful for finding (or paving) guidelines to give novel strategies to identify or manipulate convenient mutant species and /or chemical enzymes and kinases. As a consequence, the cell fate (apoptosis) can be newly interpreted.

An important goal is to improve our understanding of mutual influence between two cell networks, such as, genome guardian/emergence sub-block (p53/Mdm2) and apoptotic target genes system as recently suggested by two articles [14,15] which will be useful for improving a cellular circuitry, capable of digitally processing the p53/Mdm2 system dynamics and giving a subject for discussion about its influence on apoptosis. Both these papers deal with the mechanisms for triggering p53 pulses in response to a DNA damage. These authors showed how to obtain sustained p53 oscillations when the p53/Mdm2 negative feedback can be supplemented and integrated by a positive loop. Although negative feedback is necessary for triggering oscillations in the p53/Mdm2 system, it is not sufficient. In fact, a negative feedback loop with only two elements cannot oscillate. Moreover, observations on p53 negative feedback loop and its observed oscillations address some important questions about the roles of positive feedback loops in generating and stabilizing oscillations and how apoptosis may be triggered by repeated pulses of p53 [15].

On the basis of previous studies [25,26], where digital aerospace systems were actively controlled, in this paper a digital cell multi-layers platform is designed to pointwise evaluate cell damage checkpoints, time-dependent p53 levels and their mutual signalling. Moreover, a more complex digital cell scheme can determine different number of pulses when related to the expression of downstream genes and their evolution to give controlled time rates of considered species with desired levels of p53 and/or switch the cell fate. Then, an integration of the proposed models - independent of the type of feedback loop employed - can be achieved. The digital control system theory, mathematically expressed in terms of *state-space* theory, could unify the disparate observations and offer the possibility of investigating apoptosis once the dynamics of inner protein forms is considered.

2. Experimental Procedures

2.1 Adopted models and assumptions

In the p53/Mdm2/DNA network, both positive and negative feedbacks are involved but it is currently unknown what roles they may play in the pulsing response to DNA damage. Here, the proposed digital model reproduces (and fits quite well) the experimental data in quantitative details and, despite its simplicity, suggests new experiments that will elucidate the molecular inner mechanisms underlying oscillations in the p53/Mdm2 network.

To design suitable digital circuitry for a human single-cell, I take into account the protein forms of p53 (p53 mono-ubiquitinated, p53 poly-ubiquitinated and p53 total, *i.e.*, $p53_U$ $p53_{UU}$ and $p53_{tot}$, respectively) and Mdm2 (nuclear, cytoplasmic and phosphorylated,

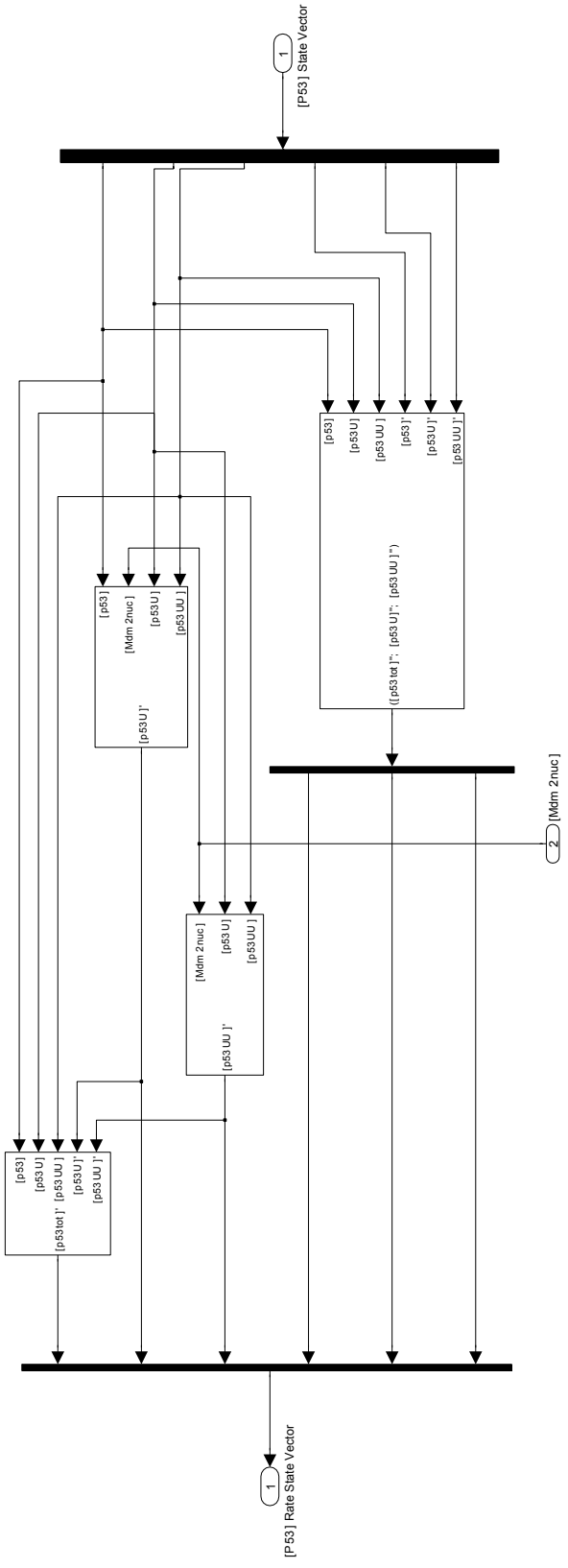

Figure 2. Cell digital dynamic matrix.

i.e., $Mdm2_{nuc}$, $Mdm2_{cyt}$ and $Mdm2_{Pcyt}$, respectively) with their time-dependence from a set of equations [14]. The problem consists of processing a set of equations in a computational space, *i.e.*, the state-space which mathematically represents all the possible conditions and combinations of the variables of the problem. Once the state-space contains the necessary equations, the numerical solution will be the task of matrix calculus. Here, the writer summarizes the biological basis upon which the present digital model is built [14].

- Mdm2 and p53 accumulate predominantly in the nucleus.
- p53 is ubiquitin-dependent degraded in a Mdm2 catalyzed reaction. Mdm2 is able to attack the first ubiquitin (other enzymes like p300 could be more efficient in further ubiquitinations) and it goes on to polyubiquitinate p53 *in vivo*. In any case, p300 is needed in further catalyzed reactions.
- p53 is intended and degraded most efficiently by the proteasome when it has at least 5 ubiquitin moieties attached. The author assumes that nuclear form of Mdm2 attaches only 2 ubiquitins to p53 (mono-/poly-ubiquitinated forms).
- Mdm2 transcription is induced by p53. The author assumes that all three forms of p53 (total, mono- and polyubiquitinated) induce Mdm2 transcription with the same level of efficiency. From a mathematical point of view, this can be modelled by a Hill function with exponent 3.
- p53 transcriptional activity is considered exploited at its utmost, *i.e.*, when 4 molecules of p53 form a tetramer.
- Cytoplasmic form of Mdm2 ($Mdm2_{cyt}$) is translocated into nucleus when it is phosphorylated by the AKT protein kinase. In the present model, this reaction transforms $Mdm2_{cyt}$ into $Mdm2_{Pcyt}$.
- $Mdm2_{Pcyt}$ freely migrates into and out of the nucleus. Nuclear volume is inside the range 1/10-/20 of the cytoplasmic one. $Mdm2_{nuc}$ concentration changes 10-20 times faster than cytoplasmic concentration. The author assumes the value of volume ratio equal to 15.
- A long pathway governs the (indirect) opposition acting by p53 to Mdm2 nuclear entry and it involves PTEN, PIP3 and AKT according to the scheme:
  $p_{53} \rightarrow$ pTEN $\rightarrow$ PIP3 $\rightarrow$ AKT $\rightarrow$ $Mdm2_{nuc} \rightarrow p_{53}$
  The author makes use of a simplified loop by taking into account that phosphorylation of $Mdm2_{cyt}$ is inhibited by $p53_{tot}$.
- In the present *in silico* simulations, a generic variable (DNA damage) DNA_{dam}, depends upon *IR* (Ionizing Radiation). The author applies 2 different values of this ionizing radiation (the first one is equal to the value in [14], and the second one is 5 times greater).
- DNA_{dam} and $p53_{tot}$ activities are governed by Michaelis-Menten kinetics.

For the single human cell circuitry design, one can digitally transform the mathematical model proposed by Ciliberto *et al.* [14] (Figures 1-2) and the model #1 by Zhang *et al.* [15] (Figure 3). Also, I digitally connect the control circuitries obtained from those models with a wiring diagram of apoptosis [15].

Making use of Simulink© software, the mathematical models of Ciliberto *et al.* [14, see Tables 1 and 3 there] and the model #1 employed by Zhang *et al.* [15] have been translated into assembled wiring digital sub-layers and the single-cell digital circuitries of the two models have been designed with respect to their biochemical interactions. The final cell digital layers run within a Matlab© computer recursive scheme based on *Linear Quadratic Regulator* (LQR) given by the control theory of digital systems. Basically, the digital circuits of this paper have been obtained once the employed mathematical models have been translated into the state-space domain and applied for a continuous time linear system (see Appendix for the control theory background, the employed biological variables and the meaning of symbols).

The LQR employed for building up the optimal control matrix, is not applied here for solving a Linear-Quadratic-Gaussian (LQG) control problem. A Gaussian-type optimal control law has not been implemented because the goal of this work was not the study about protein signals from which one deduces mean variable values (referred to Gaussian-type). The reason of this procedure is the uncertainty in linking Gaussian numerical noise properties to the “noise” rising from a DNA damage on the global numerical solutions. Thus, the LQR control scheme has been employed to demonstrate its capability to replicate the single cell dynamics during the repairing phase, which is the biological significance and also a major spin-off an acceleration of the DNA repairing action. Moreover, the biological meaning of the differences shown by this approach in its output responses and their potential testability are based upon the fact that the optimal control matrix is now built up by new reaction constants linked - in cascade - to proteins kinases under examination.

The employed control matrix derives on the control theory rules regarding the system dynamics. Even though it could be considered quite similar to a computer processing unit, it governs not only all the mathematical processes in which the considered cell species are involved but also it is conceived to numerically (and

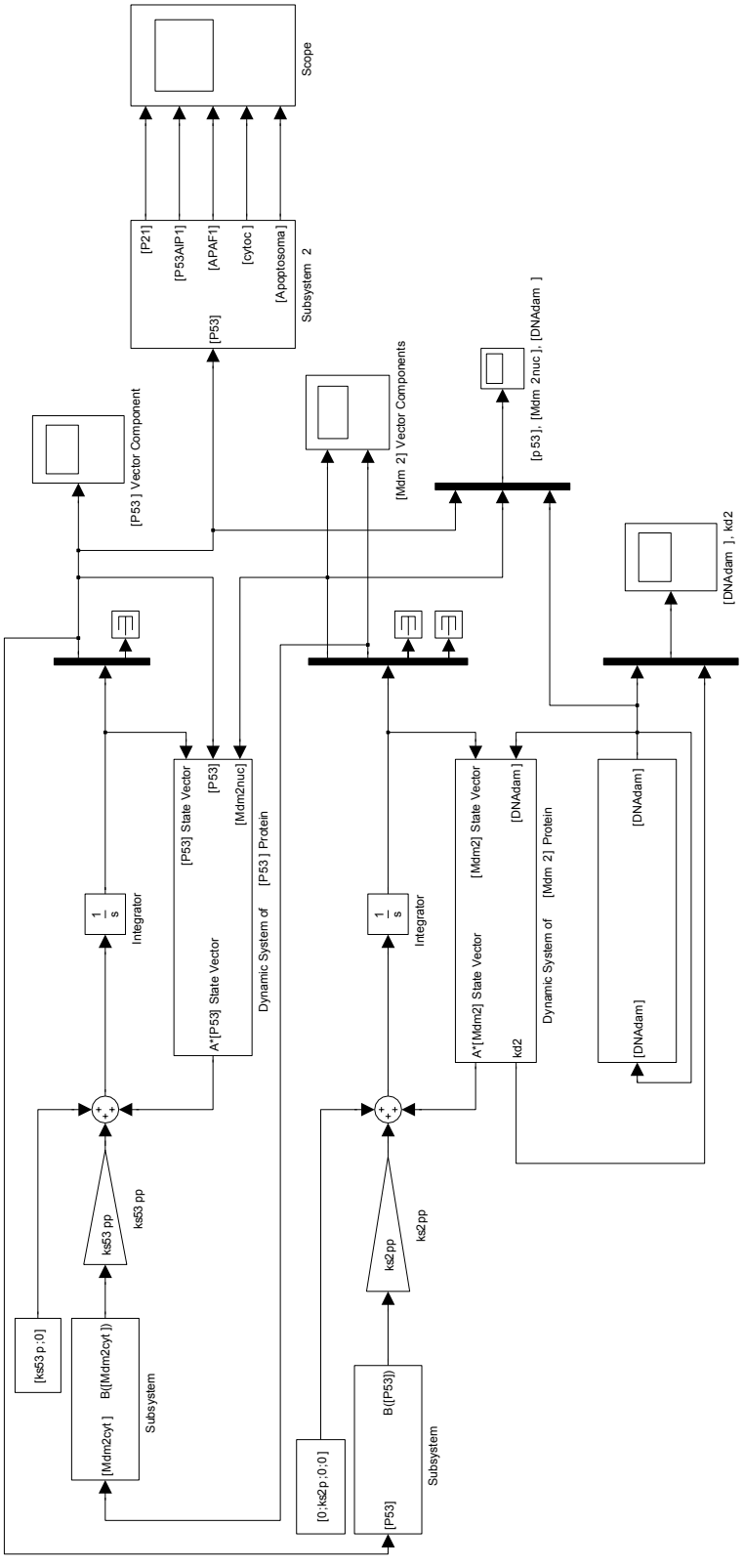

Figure 3. Cell digital circuitry (model #1 Zhang *et al.* [15]) - ks53, ks2, kd2 are the reactions constants employed to describe the time-dependency of p53, Mdm2 and DNA damage, respectively.

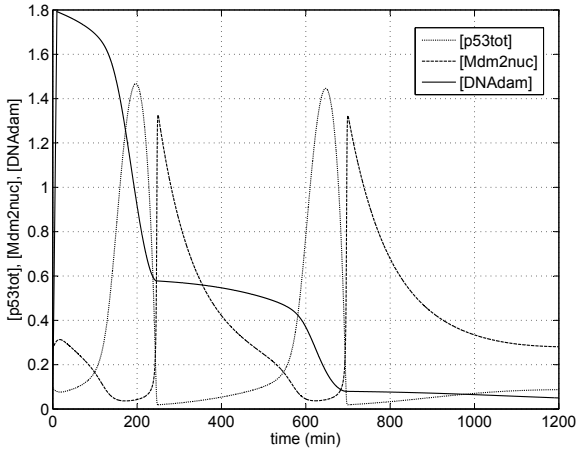

Figure 4. p53/Mdm2 pulses with DNA damage – results fit well to those of Ciliberto *et al.* [14].

digitally) accomplish the feedback control law that minimizes the (dynamic) values of the chosen protein evolution (see its close-up in Figure 2). The "structure" of the control matrix has a pure mathematical frame and its presence is needed to simulate both the cell evolutions. In normal conditions (matrix "off"), cell proteins network is described by a set of equations concerning its dynamics in "desired" condition. If the genome is under attack, emergence conditions (matrix "on") modify the proteins network signalling for accelerating the DNA repairing action.

In terms of biology, control matrix can be translated into a wild type form of one or more of the present transcription factor(s), or a different rate of phosphorylation in terms of protein terminals or kinases and/or a modified time-rate (gradient) of a downstream apoptotic protein (for example, for paving the way of finding the method for decreasing the p53-independent p21 overexpression for a steady-stable apoptosis phase).

The reliability of the digital circuitry design is ensured in two different ways. In the first model, where the digital control matrix block is switched "off" (Figure 1) one can coherently obtain the same theoretical and experimental results of literature [11,14,21] for the p53/Mdm2 dynamics when the same amount of DNA damage is imposed. Here, to avoid pictorial confusion due to the merging curves, only the present results are shown, but they replicate the previously published results (Figure 4). Moreover, the other digital circuitry can replicate the p53/Mdm2 evolution of the model #1 of Zhang *et al.* [15] as shown in Figure 5 (in state-space theory, a digital control scheme - based on the extended form of ODEs employed by [14] and [15] - should be not applicable in the state-space itself. This is due to the presence in the state-vector - as components - of both the p53 forms and its derivatives).

2.2 Model of Ciliberto *et al.*

The proposed digital circuitry coherently reproduces the experimental basis of this model, *i.e.*: a) Mdm2 and p53 are mainly degraded in the cell nucleus; b) Mdm2 is the activator of a reaction for degrading p53 in a ubiquitin-manner; c) Mdm2 attaches only two ubiquitins of p53 ($p53_U$ and $p53_{UU}$); d) three forms of p53 ($p53_U$, $p53_{UU}$ and $p53_{tot}$) induce transcription of Mdm2 in non-phosphorylated and cytoplasmic forms; e) for translocating into the nucleus, $Mdm2_{cyt}$ needs to be phosphorylated ($Mdm2_{cyt} \rightarrow Mdm2_{Pcyt}$); f) the phosphorylated cytoplasmic $Mdm2_{Pcyt}$ moves freely into and out of the nucleus; g) phosphorylation of $Mdm2_{cyt}$ is inhibited by $p53_{tot}$ in looping.

In the present study, to achieve the LQR-type (*Linear Quadratic Regulator*) kernel based optimal control scheme - a suitable manipulation of the previous set of ODEs has been done for writing and using them from the extended form into the state-space representation. In agreement with but differently from those authors [14], in the present procedure, non linear ODEs have been employed to write the set of equations with respect to the p53 protein and not to the total p53 (see Appendix).

For the present goal, we consider the level of $[Mdm2_{nuc}(t)]$ as a time variable and a matrix for the dynamic activity of p53 (time-variant). Then, Mdm2 dynamics can be expressed by a vector in the state-space. Once the proposed state-space representation gives the same results as the model of Ciliberto *et al.* [14], I assume that the matrix is such that [Mdm2nuc] is equal to a constant in such a way to implement the digital optimal control law. Using the digital scheme, several

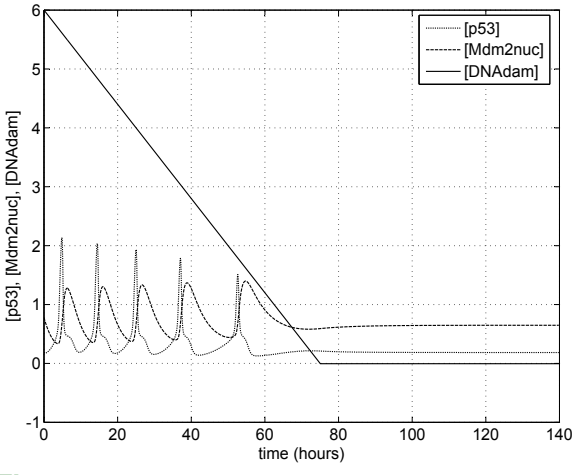

Figure 5. p53/Mdm2 pulses with DNA damage - results fit well to those of the model #1 of Zhang *et al.* [15].

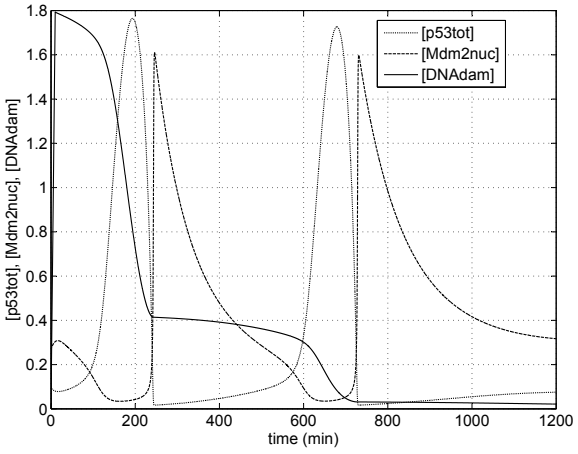

Figure 6. p53/Mdm2 pulses with DNA damage - present method (digitally controlled).

simulations have been performed and they allowed the identification of the constant value of $[Mdm2_{nuc}(t)]$ to equal to 0.1 in such a way as to obtain rates of DNA repair faster than those obtained by Ciliberto *et al.* [14].

2.3 Model #1 of Zhang *et al*.

At first, the question formulated in this work seems to be appropriate, *i.e.*, is a negative feedback loop (p53 upregulates Mdm2, which deactivates p53) sufficient to explain the observed oscillation? From a mathematical point of view, the feedback becomes positive if it is considered as a part of a complete typical digital system. Instead, if one looks at the single state-vector quantities (in feedback) containing all the forms of p53, then the feedback loop becomes "hybrid" (positive - negative) in itself, because any element of the control matrix has opposite sign with each other. In a schematic representation, one has the control matrix as follows

The optimal control matrix is derived from the

$$\underline{\underline{K}} = \begin{bmatrix} +k_{11} & -k_{12} & +k_{13} \\ \vdots & +k_{22} & -k_{23} \\ \text{sym} & \cdots & +k_{33} \end{bmatrix} \quad (1)$$

stabilizing solution of the Riccati equation (see Appendix) as a function of the dynamic matrix of the protein p53 whose elements are the reaction coefficients [14]. The above k_{ij} matrix elements are, in turn, functions of those coefficients.

In the model #1 of Zhang *et al.* [15], Mdm2 activates p53. Combined with p53-induced Mdm2 transcription, Mdm2 thereby enhances its own synthesis. The values of stable steady state concentrations are obtained once the level DNA damage is set equal to zero. When this level is different from zero, the degradation of nuclear Mdm2 increases and its concentration begins to fall. The interesting result of this model is that if the damage level is quickly repaired, the p53/Mdm2 control system develops a single-pulse response to repair the DNA damage itself. The second pulse occurs if the level of the DNA damage is relatively high. Also in this case, the designed digital circuitry faithfully reproduces the results as shown in Figure 5.

2.4 Apoptosis

Zhang *et al.* [15] show a wiring diagram of apoptosis and apply it to their model #1 (see Figure 2 in [15]). Although the above mentioned models [14,15] give different evolutions of the DNA damage repairing, the digital control theory in state-space can unify these models on the basis of the developed control matrix. Indeed, a well-suited optimal control law allows successful cell DNA damage repairing independent of its levels. Thus, I take into account the DNA damage level and the shape proposed by Zhang *et al.* [15] applied to the model of Ciliberto *et al.* [14] once it is connected to a wiring diagram of apoptosis (Figure 1 and 3).

3. Results and Discussion

The first "generation" of mathematical models for p53/Mdm2 interaction takes into account a simplified description of the negative effect of the oncogene Mdm2 on its antagonist p53, *i.e.*, the inhibition of p53 transcriptional activity and the p53 degradation through the binding of Mdm2 to the p53 itself. Lahav *et al.* [22] confirmed the p53/Mdm2 negative feedback loop oscillations. Their conclusions regarding the p53 digital behavior consist of different fractions of cells showing zero, one, two or more pulses as a function of γ-irradiation dose. The width of each pulse was 350±160 min, and the timing of the first pulse maximum was rather

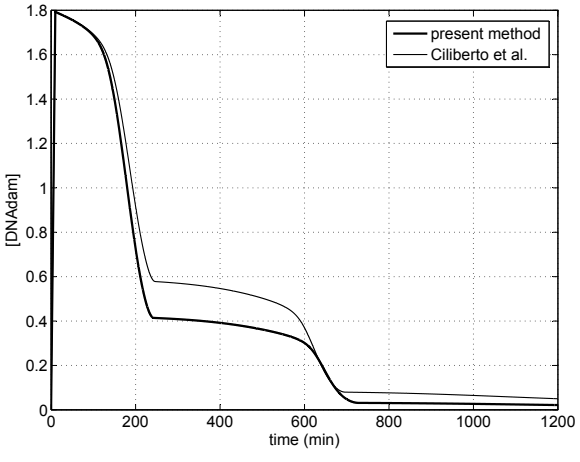

Figure 7. DNA repairing pathways comparison.

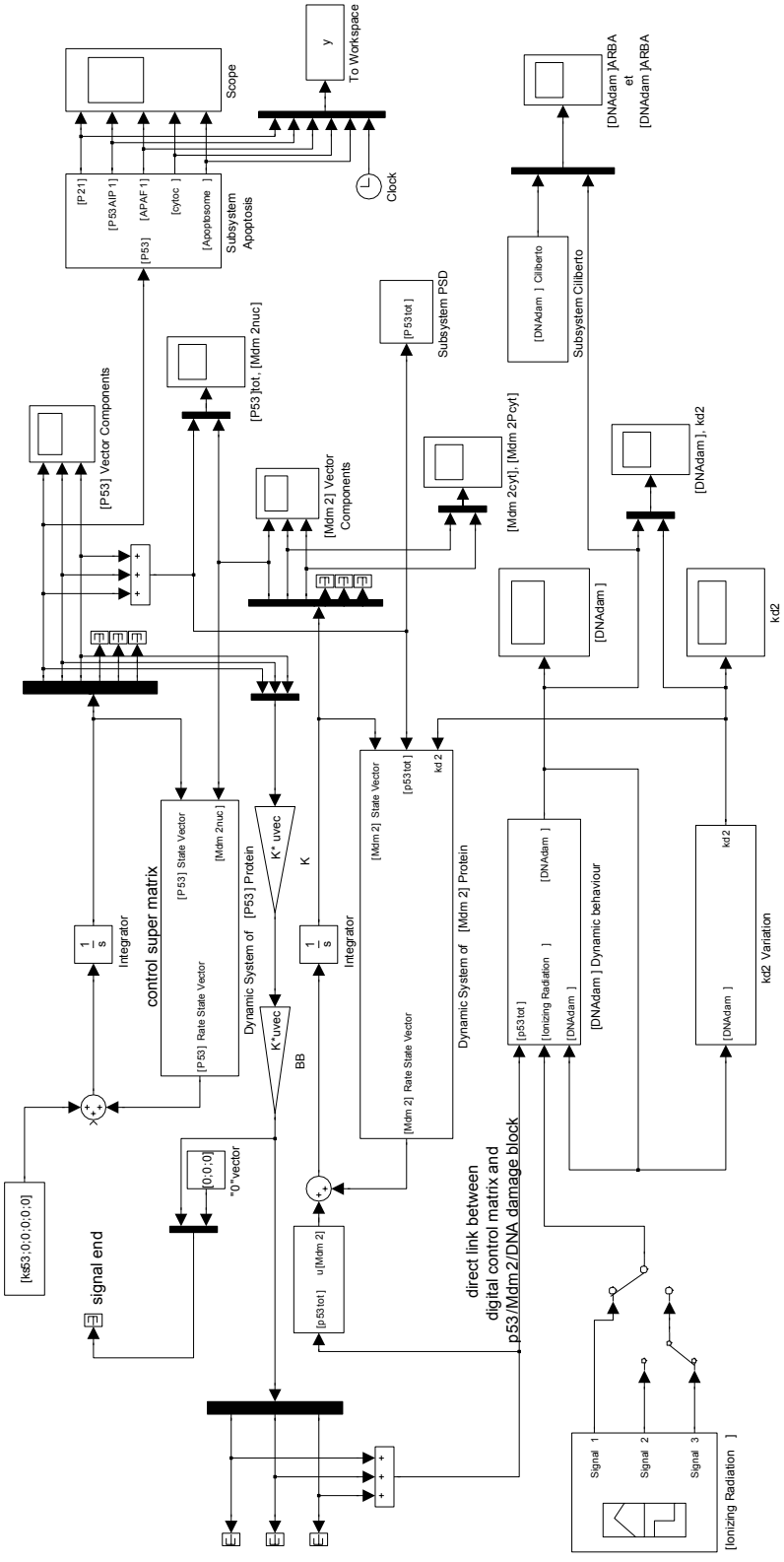

Figure 8. Human cell digital circuitry - (control matrix switched "off") LQR allows to directly chain the digital control matrix to p53/Mdm2/DNA damage block. The digital layers and blocks are the same of those in Figure 1, except the Ionizing Radiation block which performs the switch among three (or more) levels of radiation.

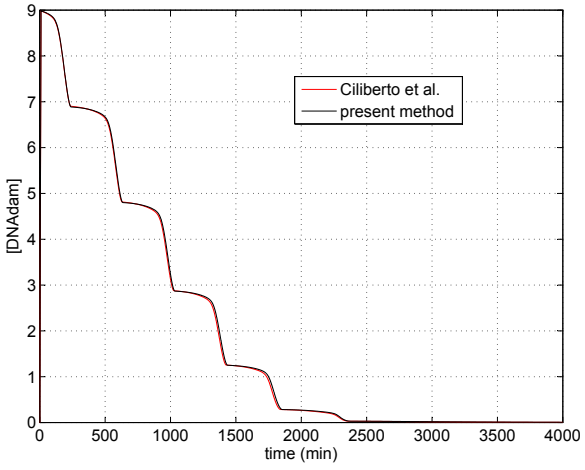

Figure 9. DNA repair pathways comparison - (*IR*=5 units).

variable (360±240 min) after damage. However, the time between the maxima of two consecutive pulses was more precise, *i.e.*, 340±100 min. Thus, they found that in the p53/Mdm2 feedback loop system, the number of pulses, but not the size or shape of each pulse, depends on the level of the input signal.

3.1 Model of Ciliberto *et al*.

Looking at the simulation output when the digital control matrix is switched "on", it can be noted that the $p53_{tot}$ and $Mdm2_{nuc}$ levels increase throughout the same timescale (Figure 6) when compared to the results when the digital control matrix was "off". Since high levels of $p53_{tot}$ involve a decrease in the DNA damage, we now switch the $[Mdm2_{nuc}]$ level to its lowest value in such a way as to obtain a positive feedback loop according to the digital control theory rules. Surprisingly, the results obtained by using *in silico* digital layers (Figure 4) change deeply (Figure 6). This could be experimentally tested if one looks at the new reaction constants of the species present as coefficients of the designed dynamic control matrix. Digital optimal control is then able to realize remarkable effects: first of all, a DNA damage repair speed faster than 50% (Figure 7) and - in cascade - a relevant variation of $p53/Mdm2_{nuc}$ dynamics.

From the comparison between Figures 4 and 6, one may deduce that the oscillation parameters of p53/Mdm2 have been modified in terms of amplitudes (higher concentrations) and interpulse (time-shift in the second pulse of about 40 min). When the initial conditions of Ciliberto *et al.* and Zhang *et al.* [14,15] are equal, the faster rate of DNA damage repair can strongly affect the response of the whole $p53/Mdm2_{nuc}$ dynamics. Moreover, the optimal control matrix is able to maintain sustained amplitudes of both p53 and $Mdm2_{nuc}$ levels.

The dual action of the control matrix has different damping effects. These effects are more evident for the second pulse of p53 and almost irrelevant for Mdm2. Each amplitude of p53/Mdm2 signal is linked to the speed of DNA repairing action in the same timespan. The first peak is triggered by the high level of DNA damage and the output responses of the uncontrolled and controlled networks have slight difference over the first timespan 0-220 min. When the second pulse triggers, the DNA local damage levels are totally different in shape (gradient) and amplitude. In the uncontrolled digital system, the gradient is confined within a range of 80 min, while in the controlled one the range becomes wider up to 120 min. In the $p53/Mdm2_{nuc}$ system, the action of the control matrix implies an overall effect, *i.e.*, an amplifying of concentrations scattered along the same timescale. Also, the global interpulse of the p53/Mdm2 network is shifted. A comparison between Figures 4 and 6 shows that the first pulse triggers at the same time interval (200-240 min), while in the digital control system, the second pulse occurs after a delay of 600+48 min. Both the uncontrolled and controlled digital circuitries show in-phase oscillations of the single protein forms, the frequency of the $[p53_{tot}/Mdm2_{nuc}]_{uncontr}$ system being equal to 3.78 10^{-5}Hz and 3.3 10^{-5} Hz for the $[p53_{tot}/Mdm2_{nuc}]_{contr}$ network.

Interpretation of these results in a biological context suggests that a controlled digital protein network (and its reaction coefficients contained in the control matrix) realizes different p53 and Mdm2 dynamics in terms of interpluses, gradients and levels of their concentrations for a faster DNA repairing action in the same timespan of the uncontrolled protein network system. The use of appropriate cell digital machinery reveals interesting perspectives for biological applications. Some of these applications can be relevant in the future: mathematical

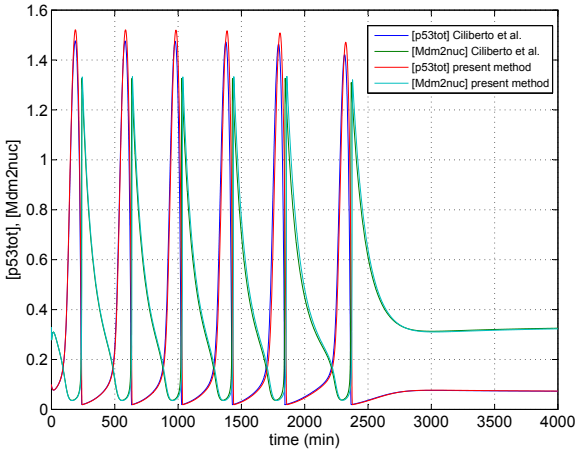

Figure 10. p53/Mdm2 pulses comparison - (*IR*=5 units).

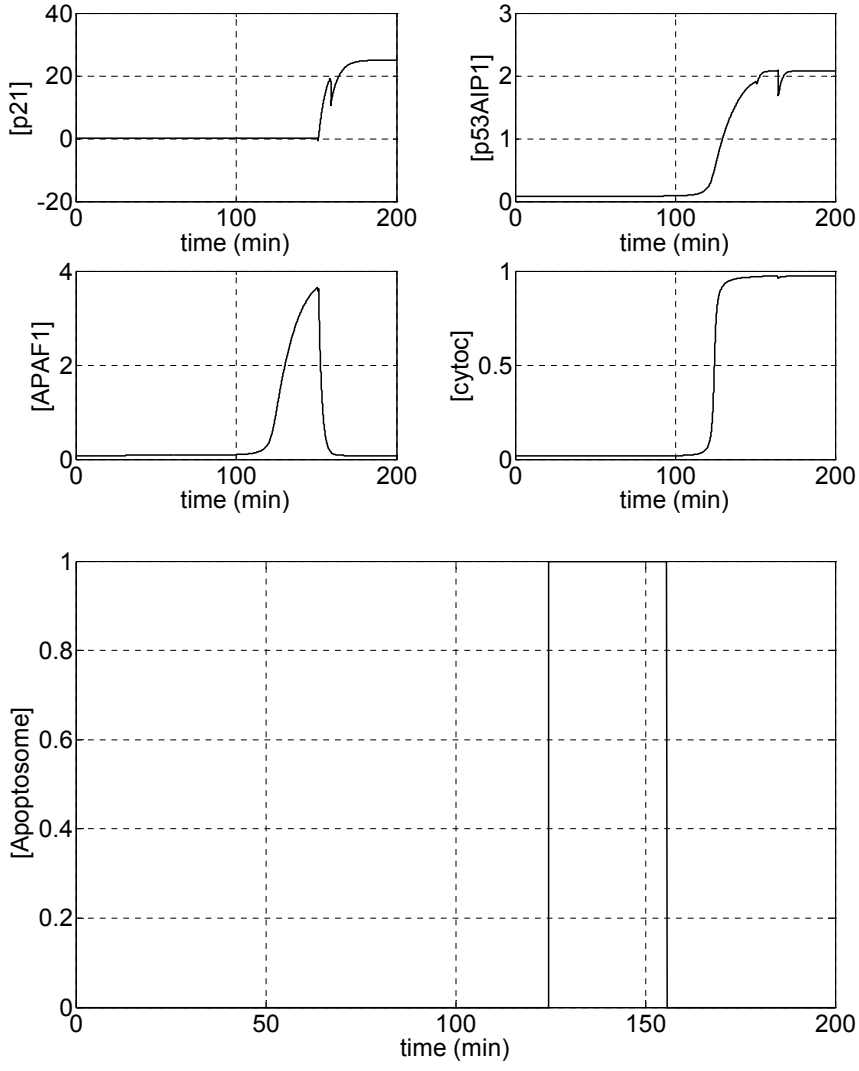

Figure 11. Species evolution in apoptosis (digitally uncontrolled).

prediction of cell behavior in absence of *in vivo* tests; future investigation for pharmacological and/or drug therapies to realize the optimal dynamics of cell proteins; proteins dynamics to inhibit or amplify some species against others; the influence of cell target species in presence of a DNA damage. Moreover, this digitally-aided cell scheme allows a wide range of regulations. For example, the proposed digital machinery is able to *in toto* replicate the cell protein dynamics when genomic damage remains constant. The dynamic control matrix can influence the DNA repair pattern in the absence of an external input from one of the proteins involved in this task. In other words, the sense and the goal of this challenge are not only the acceleration of DNA repair through a digital control matrix or to simulate cell protein evolution of a human cell under cancer attack, but to assign the task of cell defence to a mechanism governed by an integrated bio-digital system. The deduction from these assertions is that the cancer cell could not yet become aware of having the strength to play the mortal match. Having this in mind, I start to adjust the cell digital platform of Figure 1 to obtain a modified circuitry like that of Figure 8 in which the digital control matrix is directly linked to the p53/Mdm2/DNA damage system. To check the capability of the digital control matrix to externally govern the p53/$Mdm2_{nuc}$ network - independently from the natural and/or aberrant protein evolution after DNA damage - I introduce a radiation amount 5 times greater than the dose of Ciliberto *et al.* [14].

$$IR = ampl \cdot heav(0 \le t \le 10);\ ampl = 5\ units \qquad (2)$$

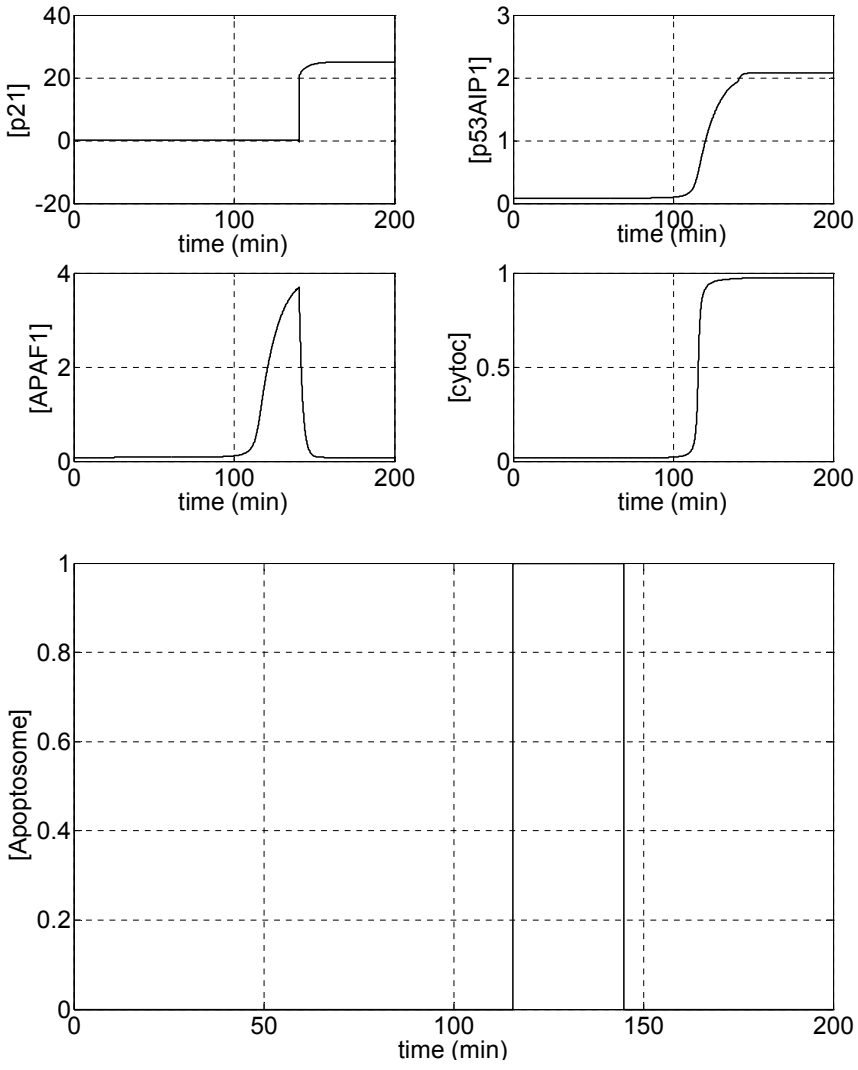

Figure 12. Species evolution in apoptosis (digitally controlled).

The simulation results shown in Figures 9-10 demonstrate that the digital control matrix - in the absence of a direct p53 signal arising from a damaged cell and only put in back-reaction to the p53 state-vector components - modulates the p53/Mdm2 oscillations until the damage is totally repaired. The number of pulses and amplitudes of the p53/Mdm2 system are now quite different from those obtained by the previous simulations. Two effects are more evident, the phase-shift between the p53/Mdm2 network (see after the second pulse in Figure 10) and the delay time after the fifth pulse. According to the local gradients of the DNA repair pattern (Figure 9), the p53/Mdm2 system undergoes steady-stable conditions. Biologically speaking, a direct connection of the control matrix to the p53/Mdm2/DNA network implies some peculiar differences. In this case, the lower repairing rate of a DNA damage is a time-dependent check point for the control matrix itself which processes a different dynamic optimal control law for the governed species. Then, p53 and Mdm2 increase their frequencies with lower concentrations levels in the same timespan (similar to [14]).

3.2 Model #1 of Zhang *et al.*

As mentioned before, this model has been converted into a digital platform circuitry in order to check the reliability of the cell digital machinery and to connect an apoptosis wiring diagram [15] to the present digital layer. In the light of the interchangeability of the previous digital control matrix - I adopt this model and its protein forms to analyze the response of the system when an apoptosis wiring diagram is considered. In this model, the initial DNA damage is repaired at a constant rate. When a wiring diagram of apoptosis is connected to this model,

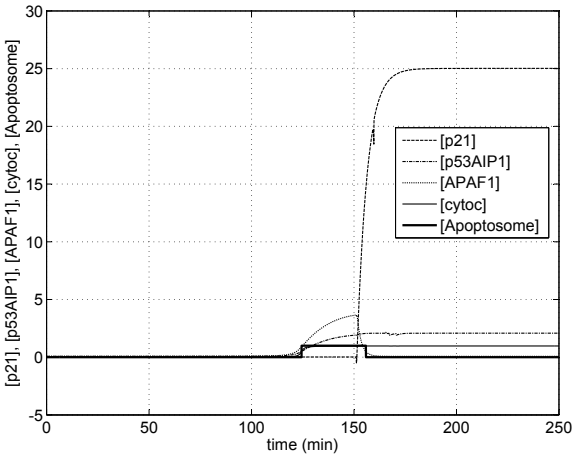

Figure 13. All at once species time history in apoptosis (digitally uncontrolled).

we consider and follow three forms of p53, (*helper, killer* and *lurker*) and their evolutions to deduce and propose a digital apoptosis mechanism. In agreement with but differently from those authors, I link their apoptosis wiring diagram - digitally converted - to cell digital circuitry having a digital control matrix (Figure 1).

3.3 Apoptosis

The decision on cell fate is now conceived and bound through the modified pulsing mechanism of p53 and other considered species when the cellular digital optimal control system is applied to an apoptosis wiring diagram (Figures 1, 3, 8). Following Zhang *et al.* [15], I take into account their apoptotic model (see Table 5 of their mentioned work). By switching the cell digital control matrix "on" or "off", the controlled ("on") and uncontrolled ("off") feedback networks give different pathways of the apoptotic species, *i.e.*, p21; p53AIP1, APAF1; and "cytoc" (as a functional of APAF1) in the apoptosome expression. This last parameter is digitally expressed by the Heaviside function, being equal to 1 (or 0) for matching (or not) the cell death. A comparison between Figures 11 and 12 shows that instabilities of apoptotic species vanish in the digital control system and, in sequence, apoptotic parameters show modified dynamics over the considered timespan in terms of signalling output responses. In the uncontrolled system, the cell fate triggers at 124.61 min and goes on for 32.3 min, while in the digital controlled network cell fate triggers at 115.3 min and remains for 27.7 min. The biological significance given by the difference shown in Figures 11-12 is that the controlled digital proteins network - acting upstream on p53/Mdm2/ DNA system and downstream on apoptotic species - alters the triggering time location of cell apoptosis phase but leaving almost unaltered the target genes rates. The species instabilities of the apoptotic network are avoided (Figure 12) and the capacity of the proposed method can pave the way for maintaining a stable apoptosis as extreme defence. In fact, the leading phase of the controlled apoptotic network and its time window could be directly tuned just in accordance with the considered species dynamics.

The previous results, when sketched all at once on the same timescale (Figures 13, 14), can bring up discussions about a suspicious behaviour of protein p21. Both the uncontrolled and controlled systems (although with different triggering and time range) show apoptotic phase just in correspondence with the inflexion point of the considered species pathways. In the proposed method, to answer a standing question in cancer dynamics, proliferation and (avoided or not) apoptosis, this novel cell digital multi-nested platform identifies a possible and common (for both the networks) unification of the proposed methods of Ciliberto and Zhang [14-15]. A digital improvement and modification of these two models can sequence and control genes dynamics of interest and it can be mathematically resumed especially for apoptosis: cell death triggers when the local gradients of the species (p21 equals to zero or is inactive) reach their maximum values at the same instant. In this case, apoptotic phase remains stable until all the considered species match their numerical maximum values. But when p21 triggers, programmed cell death phase becomes unstable and not executed. Once the local gradient of p21 reaches its transient maximum value, the cell death phase ends. Following the above mentioned procedure in which the digital control matrix is directly linked to the p53/Mdm2/DNA damage system, I come back to turn on the modified

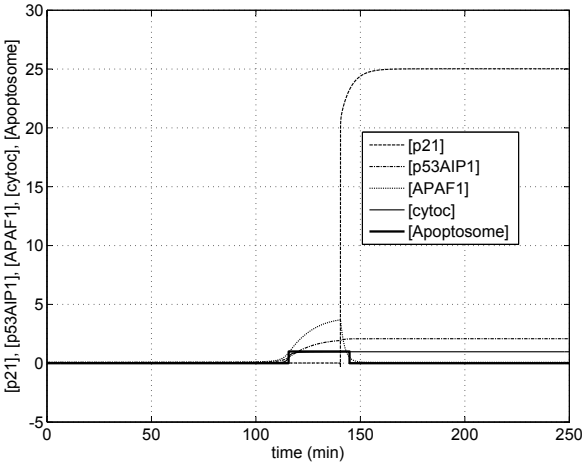

Figure 14. All at once species time history in apoptosis (digitally controlled).

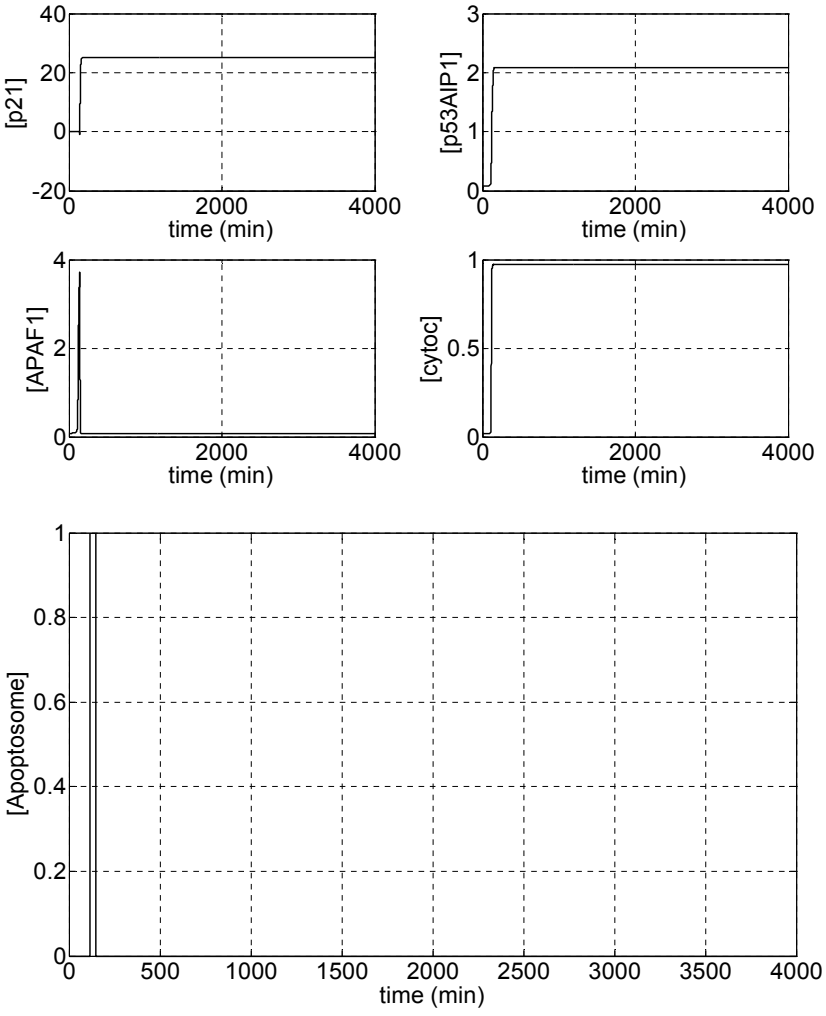

Figure 15. Species evolution in apoptosis – (*IR*=5 units (controlled)).

circuitry of Figure 8 to externally govern the p53/$Mdm2_{nuc}$ network - independently from the natural and/or aberrant protein evolution after DNA damage - and I introduce an ionizing amount 5 times greater than the dose of Ciliberto *et al.* [14]. When the DNA damage level is the same as in Figure 9, the modified circuitry scheme of Figure 8, and the digital matrix directly linked to the p53/Mdm2 network, faithfully replicates the apoptotic species of a cell in which a constant DNA damage level is considered (Figure 15).

To sum up, the evidence of designing a cell digital platform could be useful and representative in studying p53/Mdm2 evolution in a cancer cell and its fate. Limitations of the current digital design can be found in its application to a single-cell and the hypothesis of the considered number of apoptotic species (one has to remember that only some cases of [15] match cell death). The proposed cell digital layers can be improved and generalized for multi-cellular schemes and other protein complex networks including manipulations of the ionizing radiation signals and/or cell mutant genes.

Acknowledgements

The author is indebted and grateful to doctor Michael Carley for his supervision to all the recursive routines and circuitries that were processed using Matlab/Simulink™ platforms at his Department of Mechanical Engineering, University of Bath (UK). The author wishes to thank Andrea Ciliberto and Galit Lahav for their useful suggestions and the specific literary material. Marzia Sabella at the Department of Justice of Palermo (Italy) made this work possible. The author is grateful to anonymous reviewers of the manuscript for their patience and diligence.

References

[1] Ambrosi D., Preziosi L., On the closure of mass balance models for tumour growth, Math. Mod. Meth. Appl., 2002, 12, 737-754

[2] Ambrosi D., Mollica F., On the mechanics of a growing tumour, Int. J. Eng. Sci., 2002, 40, 1297-1316

[3] Ambrosi D., Mollica F., The role of stress in the growth of a multicell spheroid, J. Math. Biol., 2004, 48, 477-499

[4] Breward C.J.W., Byrne H.M., Lewis C.E., The role of cell-cell interaction in a two-phase model for a vascular tumour growth, J. Math. Biol., 2002, 45, 125-152

[5] Byrne H.M., King J.R., McElwain D.L.S., Preziosi L., A two-phase model of solid tumour growth, Appl. Math. Lett., 2003, 16, 567-573

[6] Byrne H.M., Preziosi L., Modeling solid tumours growth using the theory of mixtures, Math. Med. Biol., 2004, 20, 341-366

[7] Chaplain M., Graziano L., Preziosi L., Mathematical modelling of the loss of tissue compression responsiveness and its role in solid tumour development, Math. Med. Biol., 2006, 23, 197-229

[8] Frieboes H., Zheng X., Sun C.H., Tromberg B., Gatenby R., Cristini V., An integrated computational/ experimental model of tumour invasion, Cancer Res., 2006, 66, 1597-1604

[9] Macklin P., Lowengrub J., Nonlinear simulation of the effect of the microenvironment on tumour growth, J. Theor. Biol., 2007, 245, 677-704

[10] Panorchan P., Thompson M.S., Davis K.J., Tseng Y., Konstantopoulos K., Wirtz D., Single-molecule analysis of cadherin-mediated cell-cell adhesion, J. Cell Sci., 2006, 119, 66-74

[11] Ma L., Wagner J., Rice J.J., Hu W., Levine A., Slolovitzky G.A., A plausible model for the digital response of p53 to DNA damage, Proc. Natl. Acad. Sci. USA, 2005, 40, 14266-14271

[12] Geva-Zatorsky N., Rosenfeld N., Itzkovitz S., Milo R., Sigal A., Dekel E., et al., Oscillations and variability in the p53 system, Mol. Syst. Biol., 2006, 2, 1-13

[13] Shangary S., Wang S., Targeting the Mdm2-p53 interaction for cancer therapy, Clin. Cancer Res., 2008, 17, 5318-5324

[14] Ciliberto A, Novak B, Tyson J, Steady states and oscillations in the p53/Mdm2 network, Cell Cycle, 2005, 3, 488-493

[15] Zhang T., Brazhnik P., Tyson J.J., Exploring mechanisms of the DNA-damage response, Cell Cycle, 2007, 1, 85-94

[16] Reich C.N., Oren M., Levine A.J., Two distinct mechanisms regulate the levels of a cellular tumor antigen, p53, Mol. Cell Biol., 1983, 12, 2143-2150

[17] Ventura A., Kirsch D.G., McLaughlin M.E., David A., Tuveson D.A., Grimm J., et al., Restoration of p53 function leads to tumour regression in vivo, Nature, 2007, 445, 661-665

[18] Bates S., Phillips A.C., Clark P.A., Stott F., Peters G., Ludwig R.L., p14ARF links the tumour suppressor RB and p53, Nature, 1998, 395, 124-125

[19] Harms K.L., Chen X., The C terminus of p53 family proteins is a cell fate determinant, Mol. Cell Biol., 2005, 5, 2014-2030

[20] Bell S., Klein C., Muller L., Hansen S., Buchner J., p53 contains large unstructured regions in its native state, J. Mol. Biol., 2002, 322, 917-927

[21] Bar-Or R.L., Maya R., Segel L.A., Alon U, Levine AJ, Oren M., Generation of oscillations by the p53-Mdm2 feedback loop: a theorethical and experimental study, Proc. Natl. Acad. Sci. USA, 2000, 21, 11250-11255

[22] Lahav G., Rosenfeld N., Sigal A., Geva-Zatorsky N., Levine A.J., Elowitz M.B., et al., Dynamics of the p53-Mdm2 feedback loop in individual cells, Nat. Genet., 2004, 36, 147-150

[23] Loewer A., Lahav G., Cellular conference call: external feedback affect cell-fate decision, Cell, 2006, 124, 1128-1130

[24] Batchelor E., Mock C.S., Bhan I., Loewer A., Lahav G., Recurrent initiation: a mechanism for triggering p53 pulses in response to DNA damage, Mol. Cell, 2008, 30, 277-289

[25] Ardito Marretta R.M., Marino F., Wing flutter suppression enhancement using a well-suited active control model, J. Aero Eng., 2007, 221, 441-453

[26] Ardito Marretta R.M., Marino F., Bianchi P., Computer active control of damping fluid of a racing superbike suspension scheme for road-safety improvement spin-off, Int. J. Vehicle Des., 2008, 46, 436-450

Appendix – Control theory background

A generic time-dependent problem, involving physical variables dynamics can be translated into state-space domain. This procedure, usually employed in the systems control theory implies three powerful resources: 1) the time evolution of the variables can be followed in real time; 2) their mutual influences can be easily described (if suitable set of ordinary differential (or integral) equations is available) and 3) an optimal digital control law can be found to optimize both the recursive computational scheme and the variables dynamic responses.

A typical mathematical scheme applied for a continuous time linear system can be summarized by:

$$\dot{x} = Ax + Bu \tag{3}$$

where: $\dot{x}$ is the derivative of the state-vector, x, (containing all the variables of interest), A is the matrix of p53 transcription factor dynamics, B is the matrix of transition (LQR) input-state, u is the LQR input.

The translation of the previous set of equations requires the introduction of a quadratic cost function defined as

$$CF = \int_0^\infty (x^T Q x + u^T R u) dt \tag{4}$$

The feedback control law that minimizes the value of the cost function is

$$u = -Kx; \quad K = R^{-1}B^T P \tag{5}$$

P is found by solving the continuous time algebraic Riccati equation

$$A^T P + PA - PBR^{-1}B^T P + Q = 0 \tag{6}$$

where: Q is a semi-definite positive matrix containing, as elements, the inverse of the square maximum values of the proteins concentrations, R is a definite positive matrix containing, as elements, the inverse of the square maximum values of the input signals, K is the control matrix feedback, P is the stabilizing solution of Riccati equation (in matrix terms).

The state-vector for p53 and its concentrations shall be

$$\underline{x}(t) \triangleq \left[[p53][p53_U][p53_{UU}][\dot{p}53][\dot{p}53_U][\dot{p}53_{UU}] \right]^T \tag{7}$$

where the overdot represents the time-derivative and the subscripts U, UU identify the first-, the poly-ubiquitin protein forms and T (upper the right-hand square bracket) the transpose of the vector, respectively; while the vector

$$\underline{b} = \left[k_{s53}\ 0\ 0\ 0\ 0\ 0 \right]^T \tag{8}$$

contains the coefficient used by Ciliberto *et al.* [14]. The vector b is defined once the state-space representation is implemented for describing the input-state relationships.

I consider the level of $[Mdm2_{nuc}(t)]$ as a time variable and a matrix $\underline{\underline{P}}$ for the dynamic activity of p53 (time-variant). Mdm2 dynamics can be expressed by a vector in the state-space. Once the proposed state-space representation gives the same results as the model of Ciliberto *et al.* [14], the digital optimal control law has been implemented and based on the assumption that the matrix is such that $[Mdm2_{nuc}]$ is equal to a constant. Then, the compact expression

$$P = \left\{ \underline{\underline{P}}_{ij}; i,j = 1,2,3; p_{ij} \in \Re \right\} \tag{9}$$

(in which the symbols $\in$ and $\Re$ mean "belonging to" and range of real numbers, respectively) represents the time-invariant dynamic super-matrix. Using the digital scheme, several simulations have been performed and they allowed the identification of the constant value of $[Mdm2_{nuc}(t)]$ equal to 0.1 in such a way as to obtain a rate of DNA repair much more quickly than was obtained by Ciliberto *et al.* [14]. Once the initial conditions of stable steady-state are considered (Table 1), a digital control circuitry design can be performed through the protein [p53] state-space representation (or the equivalent [Mdm2] in feedback), *i.e.*:

$$\dot{\underline{x}}(t) = \underline{\underline{P}}\left(\left[Mdm2_{nuc}(t) \right] \right) \underline{x}(t) + \underline{b} \tag{10}$$

$$\underline{z}(t) = \left[[Mdm2_{nuc}][Mdm2_{cyt}][Mdm2P_{cyt}][\dot{M}dm2_{nuc}][\dot{M}dm2_{cyt}][\dot{M}dm2P_{cyt}] \right]^T \tag{11}$$

$$\dot{\underline{z}}(t) = \underline{\underline{M}}\left(\left[p53_{tot}(t) \right], k_{d2}(t) \right) + \underline{c}\left(\left[p53_{tot}(t) \right] \right) \tag{12}$$

$$\underline{c} = \left[0\ f\left(\left[p53_{tot}(t) \right] \right) 0\ 0\ 0 \right]^T \tag{13}$$

where $[Mdm2_{nuc}(t)]$ defines the time-dependent oncogene concentration rate in nuclear form during the DNA repairing action. $[Mdm2_{cyt}]$ and $[Mdm2_{Pcyt}]$ are the time-dependent oncogene concentration rates in cytoplasmic and phosphorylated forms, respectively; $k_{d2}(t)$ is the rate constant for degradation of $[Mdm2_{nuc}(t)]$; the time-dependent expression $f([p53_{tot}(t)]$ represents the Hill function. All the blacked quantities above mentioned are denoting time varying scalar quantities. $\underline{\underline{P}}$ and $\underline{\underline{M}}$ identify the dynamic matrices for the transcription factor p53 and the Mdm2 oncogene, respectively. They are obtained once a state-space representation model has been carried out by the extended expression of the ODEs employed by [14].

The subscripts nuc, cyt and Pcyt identify nuclear, cytoplasmic and phosphorylated cytoplasmic protein forms, respectively; while the vector in Eq. 13 contains the known function f [14]. More precisely, some auxiliary matrices have been employed as follows:

$$\underline{\underline{K}} = LQR\left(\underline{\underline{P}}, \underline{\underline{BB}}, \underline{\underline{Q}}, \underline{\underline{R}}, \right) \tag{14}$$

where $\underline{\underline{K}}$ is the digital optimal control law matrix obtained by resolving the Riccati's equation, $\underline{\underline{BB}}$ the input-state transition matrix, while the positive definite matrices

Parameters	Description	Values
f	Hill function	
$q_{ij} \in \underline{\underline{Q}}$	Bryson rule matrix diagonal elements (LQR)	1 min^{-1}
$r_{ij} \in \underline{\underline{R}}$	Bryson rule matrix diagonal elements (LQR)	0.5 min^{-1}
k_{s53}	Rate of overexpressed $p53_{tot}$	0.055 min^{-1}
k_{d53}	Rate of $p53_{UU}$ degradation	8 min^{-1}
k'_{d53}	Rate of $p53_{tot}$ degradation	0.0055 min^{-1}
k_f	Rate of $Mdm2_{nuc}$-dependent $p53_U$ degradation	8.8 min^{-1}
k_r	Translation rate of $p53_{UU}$	2.5 min^{-1}
k_{DNA}	Rate IR-dependent DNA damage	0.18 min^{-1}
k_{dDNA}	Rate of $p53_{tot}$ degradation-dependent DNA damage	0.017 min^{-1}
IR	Ionizing Radiation	
J_{DNA}	State variable in Hill function for DNA repair	1
ampl	IR dose amplitude unit	1

Table 1. Parameters for the p53/Mdm2 network model

$\underline{\underline{Q}}$ and $\underline{\underline{R}}$ are defined in such a way their diagonal contains the setting values to obtain suitable control law for a desired protein forms dynamics. The pre-multiplying factors of the matrices $\underline{\underline{Q}}$ and $\underline{\underline{R}}$ have been imposed in such a way the pattern of the components of the state-vectors $\underline{x}(t)$, $\underline{z}(t)$ and the DNA damage are quite similar to those of [14], while the optimal control matrix has to accomplish the task to accelerate the DNA repair process according to the equation:

$$\frac{d[DNA_{dam}]}{dt} = k_{DNA}[IR] - k_{dDNA}[p53_{tot}]\frac{[DNA_{dam}]}{J_{DNA} + [DNA_{dam}]} \quad (15)$$

in which *IR* represents the functional of the imposed radiation dose; while k_{DNA}, k_{dDNA}, DNA_{dam}, J_{DNA} represent the (direct) rate constant linked to ionizing radiation, the direct constant rate linking DNA damage to the rate of transcription factor $p53_{tot}$, the amount of damaged DNA and the Michaelis constant of $p53_{tot}$-dependent DNA damage, respectively.

The system of differential equations obtained must be processed and resolved, *i.e.*:

$$\begin{cases} \underline{\underline{P}}^T\underline{\underline{S}} + \underline{\underline{S}}\underline{\underline{P}} - (\underline{\underline{S}}\underline{\underline{B}}\underline{\underline{B}})\underline{\underline{R}}^{-1}(\underline{\underline{B}}\underline{\underline{B}}^T) + \underline{\underline{Q}} = 0 \\ \underline{\underline{K}} \equiv \text{optimal control law} = \underline{\underline{R}}^{-1}(\underline{\underline{B}}\underline{\underline{B}}^T\underline{\underline{S}}) \end{cases} \quad (16)$$

from the first equation of the above system, one obtains the Riccati stabilizing solution $\underline{\underline{S}}$, and the second equation is then solved.

The optimal control matrix terms being a function of the following parameters:

$$\begin{cases} \underline{\underline{K}} = \{k_{ij} \in \Re / k_{ij} = f(q_{ij}, r_{ij}, [Mdm2_{nuc}], k_f, k'_{d53}, k_{d53}, k_r) \\ [Mdm2_{nuc}] = \text{const} \\ q_{ij} \in \underline{\underline{Q}} \\ r_{ij} \in \underline{\underline{R}} \end{cases} \quad (17)$$

where k_f, k'_{d53}, k_{d53} and k_r are the translation rates of $[Mdm2_{nuc}]$, $[p53_{tot}]$, $[p53_{UU}]$ and the translation rate of $[p53_{UU}]$-dependent $[p53_U]$, respectively.

Easy mathematical manipulation of the equation of p53 yields:

$$\frac{d}{dt}[p53_{tot}] = \frac{d}{dt}[p53] + \frac{d}{dt}[p53_U] + \frac{d}{dt}[p53_{UU}] \quad (18)$$

and then one obtains:

$$\begin{aligned} &\frac{d}{dt}[p53] = -k'_{d53}[p53] - \left(k'_{d53}[p53_U] + \frac{d}{dt}[p53_U]\right) + \\ &-\left((k'_{d53} + k_{d53})[p53_{UU}] + \frac{d}{dt}[p53_{UU}]\right) \\ &\frac{d}{dt}[p53_U] = k_f[Mdm2_{nuc}][p53] - (k'_{d53} + k_r + k_f[Mdm2_{nuc}])[p53_U] + k_r[p53_{UU}] \\ &\frac{d}{dt}[p53_{UU}] = k_f[Mdm2_{nuc}][p53_U] - (k'_{d53} + k_{d53} + k_r)[p53_{UU}] \end{aligned} \quad (19)$$

Now, if the optimal control law is applied, further terms belonging to the matrix $\underline{\underline{K}}$ must be added, and then the extended form of the final system of equations is obtained. Rearranging the system (eq. 19), one comes to:

$$\begin{aligned} &\frac{d}{dt}[p53] = -(k'_{d53} + k_f[Mdm2_{nuc}])[p53] + k_r[p53_U] + k_{s53} + \sum_{n=1}^{3} k_{1,n}x_{n,1} \\ &\frac{d}{dt}[p53_U] = k_f[Mdm2_{nuc}][p53] - (k'_{d53} + k_r + k_f[Mdm2_{nuc}])[p53_U] + \\ &+k_r[p53_{UU}] + \sum_{n=1}^{3} k_{2,n}x_{n,1} \\ &\frac{d}{dt}[p53_{UU}] = k_f[Mdm2_{nuc}][p53_U] - (k'_{d53} + k_{d53} + k_r)[p53_{UU}] + \sum_{n=1}^{3} k_{3,n}x_{n,1} \end{aligned} \quad (20)$$

For the adopted values of the matrix elements, k_{ij}, see Table 2. Once the LQR has been performed, those elements were obtained by a linear combination of the rate constants shown in Table 1.

Matrix elements	Description	Constant
k_{11}	Digital optimal control matrix element	0.0023 min^{-1}
$k_{12} = k_{21}$	Digital optimal control matrix element	0.0017 min^{-1}
$k_{13} = k_{31}$	Digital optimal control matrix element	0.0004 min^{-1}
k_{22}	Digital optimal control matrix element	0.0015 min^{-1}
$k_{23} = k_{32}$	Digital optimal control matrix element	0.0004 min^{-1}
k_{33}	Digital optimal control matrix element	0.0001 min^{-1}

Table 2. Optimal control matrix coefficients